Hydrodynamics in subsurface CO2 storage: Tilted contacts and increased storage security

Hydrodynamics in subsurface CO_2 storage: Tilted contacts and increased storage security

N. Heinemann[a], R.J. Stewart[a], M. Wilkinson[a], G.E. Pickup[b], R.S. Haszeldine[a]

[a]School of GeoSciences, University of Edinburgh, Edinburgh EH9 3JW, Scotland, UK

[b]Institute of Petroleum Engineering, Heriot-Watt University, Riccarton Campus, Edinburgh EH14 4AS, UK

Abstract

Hydrodynamic aquifers with horizontal variations in overpressure and brine flow have been reported from sedimentary basins worldwide. In a hydrodynamic aquifer pore-waters flow in the direction of overpressure reduction, whereas trapped hydrocarbons remain static. The main effect of this pressure disequilibrium in the aquifer is a tilt of the free water levels (FWL) in the direction of lower overpressure.

Although the impact of hydrodynamics on the petroleum system is established in the oil industry and provides important information for exploration and field development, the interaction of CO_2 storage and hydrodynamic flow has hardly been investigated. Supercritical CO_2 has a density comparable with oil densities in known hydrodynamic systems in the North Sea. Hence, a tilted CO_2-water FWL is expected and has to be taken into account during the planning of CO_2 storage. Hydrodynamic spill points will replace structural spill points as a parameter in CO_2 storage capacity calculations.

Storage security is dependent on CO_2 dissolution rates, among other factors. The more effectively CO_2 dissolves into brine the more CO_2 will be permanently stored in the subsurface. Numerical simulations show that CO_2 storage in hydrodynamic aquifers enhances the dissolution of CO_2 compared with a static regime. When CO_2 dissolves into brine, the brine density increases and the CO_2-saturated brine sinks to the bottom of the reservoir and is replaced by under-saturated brine. In a hydrodynamic system the brine saturated with CO_2 will be removed more effectively from the CO_2-brine interface. Hence, CO_2 comes in contact with more under-saturated brine and dissolves at a greater rate.

The presence of hydrodynamic flow in a reservoir requires a high degree of understanding but research on oil reservoirs has proven that it is an uncertainty that can be adequately characterized. For long term CO_2 storage operations hydrodynamic flow can even be an opportunity for more secure CO_2 storage.

1. Introduction

The capture of CO_2 from large scale emitters such as combustion power stations and the subsequent storage in the subsurface is considered as a significant contribution to mitigate rising CO_2 concentrations in the atmosphere (Lovell, 2011; IPCC, 2014). The most promising storage targets are depleted hydrocarbon reservoirs, where CO_2 will be injected into structural traps and displace the in-situ pore fluid and saline aquifers. The storage targets should ideally be connected to an open pressure system so that injection induced overpressure can dissipate and does not compromise the sealing formations (Zhou et al., 2008).

This study investigates the injection of CO_2 into aquifers which are open and have a constant flow of brine due to horizontal variations in overpressure. It focusses on two aspects: Firstly, will the horizontal variation in overpressure tilt the CO_2-water free water level (FWL) in a similar way it tilts the oil-water FWL in oil fields with hydrodynamic aquifers? And secondly, will the hydrodynamic flow increase storage security by enhancing the dissolution rate of CO_2 into brines? The examples and data used in this study are from the North Sea but the conclusions are relevant for potential CO_2 storage operations in hydrodynamic aquifers worldwide.

2. Hydrodynamic flow in the North Sea

In this study, hydrodynamic flow in a permeable formation is defined as fluid flow as a consequence of horizontal variations in overpressure, i.e. a change in overpressure across a horizontal distance independent of depth. Overpressure is defined to be any pressure higher than the hydrostatic pressure as defined by a hydrostatic gradient. In a hydrostatic or uniformly over-pressured aquifer, no horizontal variations in overpressure exist and the pore fluid remains static. By contrast, the horizontal variation in overpressure in a hydrodynamic aquifer is gradual. Natural reasons for the generation of overpressure have been discussed in various papers (e.g. Bjoerlykke, 1997; Swarbrick and Osborne, 1997) and in the North Sea are thought to relate to processes such as burial compaction disequilibrium, thermal cracking of gas and associated volume change disequilibrium and thermal expansion of water leading to a volume change disequilibrium. Overpressure in permeable formations can lead to the flow of brine in response to horizontal variations in overpressure. If a less dense second phase such as oil is trapped within a hydrodynamic aquifer the free water level (FWL), the point of zero capillary pressure between oil and water, will tilt. Tilted FWLs of oil and water due to horizontal variations in overpressure were first described by Hubbert (1953, 1967). Often the terms FWLs and oil-water contacts (OWC) are used synonymously because they are usually close to one another in high permeability reservoirs. However, the principle of hydrodynamic tilting applies strictly to FWLs and only by extension to OWCs (Dennis et al., 2000). In this study, we will use the term FWL because it covers all 'contacts' between brine and a second phase (oil, gas and supercritical CO_2).

Both varying FWLs and lateral pressure changes within aquifers can be interpreted in different ways. Horizontal variations in overpressure in reservoirs are often interpreted to be a result of fault compartmentalization or other low permeability barriers which disconnect an otherwise open flow system (Dennis et al., 2005). However, the unique characteristics of a hydrodynamic system are horizontal variations in overpressure in the brine in combination with no overpressure gradient in the hydrocarbon leg (Dennis et al., 2000).

The tilt of the FWL in a hydrodynamic system is a response of the less dense phase to the pressure disequilibrium of the brine and is not caused by friction associated with the water movement. Hence the tilt per km can be expressed with the horizontal variation in overpressure and the phase density contrast (Dennis et al., 2000):

$$dz/dx = \frac{dp/dx}{dp/dh_{(w-h)}}$$

where *dz/dx* is the dip of the FWL per unit length, *dp/dx* is the horizontal variation in overpressure expressed as pressure per unit length, and $dp/dh_{(w-h)}$ is the difference in vertical pressure gradients between the two phases expressed as pressure per unit column height.

Hydrodynamic flow and tilted FWLs have been reported from various parts of the world, for example from Cretaceous aquifers of Southwestern Saskatchewan (Melnik and Rostron, 2011); the South Caspian Sea (Tozer and Borthwick, 2010); Western Alberta Sedimentary Basin (Bachu & Underschultz, 1993), the Gulf of Mexico (Dias et al., 2010; Green et al., 2014) and from the North Sea.

In the Norwegian North Sea, varying FWLs in the Jurassic Ula field were interpreted by O'Connor et al. (2011) to be a result of hydrodynamic flow towards a nearby salt diaper which acts as a pressure valve. They calculated a horizontal variation in overpressure across the field of 47 psi/km (324 kPa/km) and a tilt of the FWL of 93 m/km for the oil field. Megson (1992) and Thomasen & Jacobsen (1994) described tilted fluid contacts in the Kraka and the Dan fields, two oil fields in the Cretaceous chalk of the Danish Central Graben. Additionally, Dennis (2000) described varying oil-water FWL in the Valhall and the Hod field, two Cretaceous chalk fields located in the Central North Sea. According to his interpretation, the accumulations are in pressure communication and a horizontal variation in overpressure of approximately 7 psi/km (48 kPa/km) across the field leads to a tilt of 15 m/km. The most prominent example of tilted FWLs in the North Sea is probably the Pierce field, a Paleocene sandstone reservoir located in the Central North Sea (Dennis et al., 2000; Birch & Haynes, 2003). Pressure data from well tests show a horizontal variation in overpressure of 45 psi/km (310 kPa/km) across the field and wireline data identified a FWL of more than 300 m vertical relief (90 m/km) towards WNW.

The Pierce field is interpreted to be a part of a regional scale hydrodynamic system in the Paleocene Forties Sandstone Member of the Central North Sea (Cayley 1987; Dennis 2000). Robertson et al. (2013) plotted 74 pressure measurements taken in the Forties Sandstone which show that overpressure increases towards the southeast, in the direction of increasing distance from the sediment source and decreasing gross reservoir thickness. In the northwestern part of the study area, where the sands are shallowest and pressures are close to hydrostatic, it is inferred that fluids drain laterally into the shelf sandstones belonging to the Dornoch Formation (Robertson et al., 2013).

3. Tilted FWLs in a CO_2-water system

Hydrodynamics has been accepted in the oil industry as a theory that can provide important information to improve exploration success and the field development process. There are two ways to determine the tilt of a FWL. Firstly, by comparing OWC interpreted from wireline data drilling reports (assuming that changes of the OWCs and the FWLs are similar), and secondly, by calculation of the tilt using pressure data and fluid densities from multiple wells. If the tilt of the FWL is known, structural spill points, locations which control the maximum extent of a hydrocarbon accumulation, must be replaced by 'hydrodynamic spill points' (Green et al., 2014). Depending on the degree of tilt and on the field architecture, the updated spill points can change the maximum volume of a hydrocarbon accumulation significantly.

So far previous research has focused on the impact of hydrodynamic flow on oil fields because oil densities are generally closer than natural gas to subsurface brine densities and the tilt of the FWL will be more prominent. There has been little interest in tilted FWL in gas fields. Natural gas in reservoir rocks, of which the majority is methane, has a relatively low density of less than 0.2 g/cm^3 under normal reservoir conditions (Setzmann & Wagner, 1991). Due to the large density difference between methane and brine under subsurface conditions, no significant tilts are expected in gas reservoirs even if a strong horizontal variation in overpressure is present. However, CO_2 does not behave like methane in the subsurface. At temperature and pressure conditions higher than 31.1°C and 7.39 MPa, respectively, a phase change takes place and CO_2 will be present as a supercritical fluid with a liquid like density (IPPC, 2005). The rapid increase in density provides the potential for efficient underground storage but it decreases the density contrast between brine and stored CO_2. Since a reduced density contrast between two phases increases the tilt of the FWL, CO_2 in the subsurface is much more affected by hydrodynamic flow than e.g. methane. This effect was modelled by Lindeberg et al. (2000) for the potential hydrodynamic flow in the Utsira CO_2 storage site (Norway). They found a hydrodynamic flow rate of 3 m/year will tilt the CO_2 brine contact and displace the CO_2 plume.

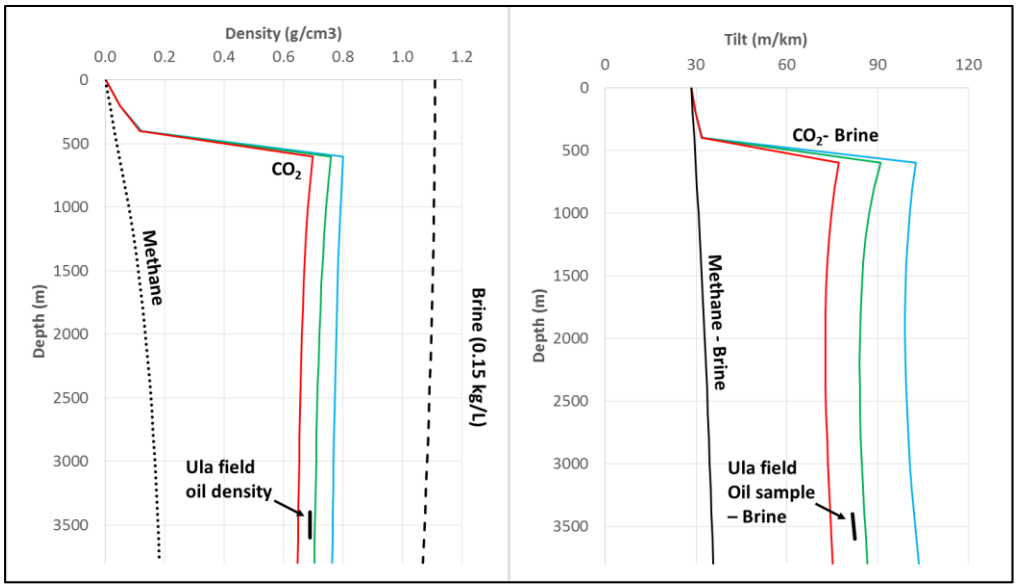

Figure 1: (left) The graph shows the density change with depth for a selection of reservoir fluids for, if not stated otherwise, a vertical temperature gradient of 30°C per km. Oil density is taken from the North Sea Ula Field (O'Connor et al., 2011) and plotted for the depth range investigated in O'Connor et al., 2011. Methane and brine densities are calculated using Setzmann and Wagner (1991) and Batzle and Wang (1992), respectively. CO_2 Density calculated for three different temperature gradients (red – 35°C/km; green – 30°C/km; blue - 25°C/km) are also shown. The graph shows that at reservoir depth the density of supercritical CO_2 is within the range of the density of the oil. (right) The graph shows the tilt of FWLs with depth of the same reservoir fluids in the presence of brine (0.15 kg/l). The horizontal variation in overpressure across the field is assumed to be 310 kPa/km, similar to the horizontal variation in overpressure identified in the Pierce and the Ula Field. Methane has a low density and the gas-water FWL shows a tilt of ~30 m/km. The tilt of the oil-water FWL using oil densities from the Ula Field is approximately 80 m/km. Also shown is the potential tilt of a CO_2-water FWL calculated for the three temperature gradients. When CO_2 is present as a gas phase, the tilt is similar to the tilt of a methane-brine system. Once it is in supercritical state, potential tilts are comparable with the tilts in known hydrodynamic oil fields. Hence, if tilted oil-water FWL are present, CO_2-water FWL will tilt too.

Figure 1 shows the density changes of brine (0.15 kg/l) calculated using Batzle and Wang (1992) and methane densities calculated using Setzmann and Wagner (1991). The oil density example was taken from O'Connor et al. (2011) and represents the density of oil in the Ula field. Also shown are CO_2 densities for three temperature gradients (25/30/35°C/km) and similar pressure conditions, calculated using the Span & Wagner equation of state (Span and Wagner, 2006). The hydrostatic pressure

conditions used to calculate the density for methane and CO_2 were determined by combining the atmospheric pressure and the weight of the overlying water column based on brine density calculated using Batzle and Wang (1992) and a temperature gradient of 30°C/km and a surface temperature of 5°C.

Figure 1 shows that within realistic temperature conditions, supercritical CO_2 in the subsurface has a fluid density similar to the oil in the Ula field. Since the FWL in the Ula field is significantly tilted, a potential CO_2-brine FWL will also be tilted under the same conditions. Figure 1 also shows the tilt of the FWL for CO_2, methane and oil with a horizontal variation in overpressure of 310 kPa/km, which is comparable with hydrodynamic conditions at the Ula and the Pierce field (O'Connor et al., 2011; Dennis et al., 2000). The assumed salinity of the brine is 0.15 kg/l. As it can be seen, the CO_2-water FWL will be tilted by comparable degrees as the present oil-water FWL. Lower temperatures increase CO_2 and brine densities at different rates, therefore there is a net decrease in the density difference between the injected CO_2 and the brine and therefore tilting is enhanced. The density of brine is barely affected by temperature and pressure but a decrease in salinity reduces the brine density and also decreases the density difference. Hence, all other things being equal, lower salinities enhance the tilting too.

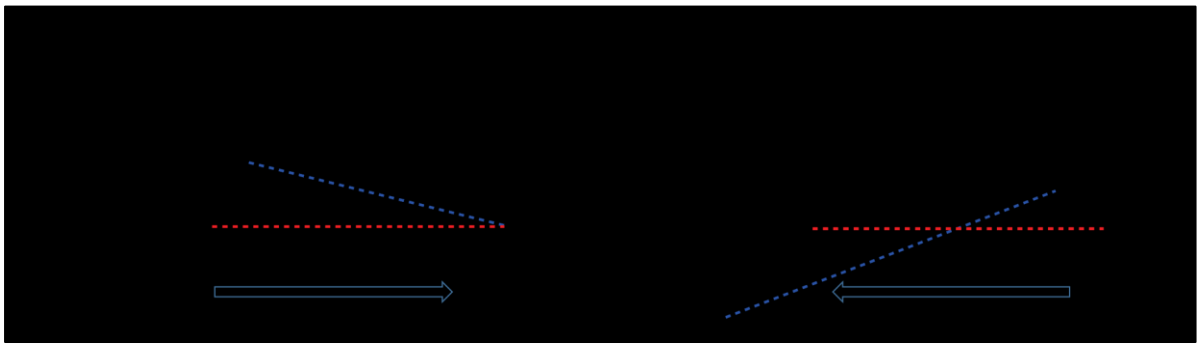

Figure 2: Schematic figure to demonstrate how a horizontal variation in overpressure may increase or decrease CO_2 storage capacity estimations based on hydrostatic conditions. If the FWL of a CO_2-brine system is tilted due to hydrodynamic flow (blue dotted line), it depends on the architecture of the trap if structural spill points still control the storage capacity (scenario A) or whether they have to be replaced by hydrodynamic spill points (scenario B) for capacity estimations.

The data presented in Figure 1 show that if hydrodynamic flow is present, it will tilt the FWL in an engineered CO_2 storage operation. Just as the volume of potential hydrocarbons in place can be highly dependent on the interaction of the reservoir architecture and the geometry of the FWL, so does the storage capacity of free phase CO_2 (Figure 2). However, the tilting of the FWL does not happen instantly and the CO_2 plume will find its final shape long after injection has ceased. The increase of CO_2 storage capacity is therefore theoretical; injection might have to take place over a potentially infeasibly long time period to slowly use space provided by the tilting. It is also important to point out that the capacity will only be altered by hydrodynamic flow if the initial capacity estimation is based on structural trapping defined by structural spill points only, and not for example by a limiting increase in pore fluid pressure. Additionally, the placement of CO_2 injection wells would have to be reconsidered to use the full storage potential of a depleted hydrocarbon field or a structural trap in a saline aquifer.

4. Enhanced CO_2 dissolution in hydrodynamic reservoirs

One of the first chemical processes occurring after CO_2 injection has started is the dissolution of CO_2 into the pore water. The dissolution rate is an important parameter to determine storage security because the faster the CO_2 dissolves, the quicker the volume of free CO_2 decreases. This reduces the risk of CO_2 migrating out of the storage site and also reduces the buoyancy pressure on the cap rock. The dissolution of CO_2 into saline water leads to an increase in the density of the liquid phase. When CO_2 dissolves at the CO_2 water interface, the CO_2-saturated aqueous phase sinks, and as it does so, under-saturated brine rises and comes into contact with the CO_2 (Ennis-King and Paterson, 2005; Ghanbari et al., 2006).This convection process enhances dissolution and therefore enhances storage security.

4.1. Methodology

To investigate the impact of hydrodynamic flow on the dissolution rate, the injection of CO_2 into a hydrodynamic system was simulated using the reservoir engineering software Eclipse100 (Schlumberger; Figure 3). The modeled aquifer has a top depth of 2000 m TVD with an anticline in the center with a top depth of 1900 m TVD and a reservoir temperature of 60°C. The model extent is 6400 m by 3200 m with a constant thickness of 150 m and the bottom seal mirrors the shape of the top seal. The horizontal width of the anticline is 2400 m. The computed pore volume of the anticline is 0.021 km^3. The number of grid cells is 64x32x10. A well injects CO_2 into the top two cells (equivalent to a 30 m perforation) of an anticline in the center of the mesh. A set of 11 wells inject water over the entire thickness of the reservoir across one end of the model. Simultaneously, 11 production wells at the other end of the model, controlled by a bottom hole pressure upper limit of 21,000 kPa, produce water to maintain a constant water flow and a constant pressure gradient. Due to the varying water injection rates, the average pressure of the simulations increases slightly between model runs with increasing horizontal variations in overpressure. The absolute average water pressure for the nearly hydrostatic model and the 144 kPa/km model at the end of the run time is 20,695 kPa and 21,179 kPa, respectively, a difference of 484 kPa.

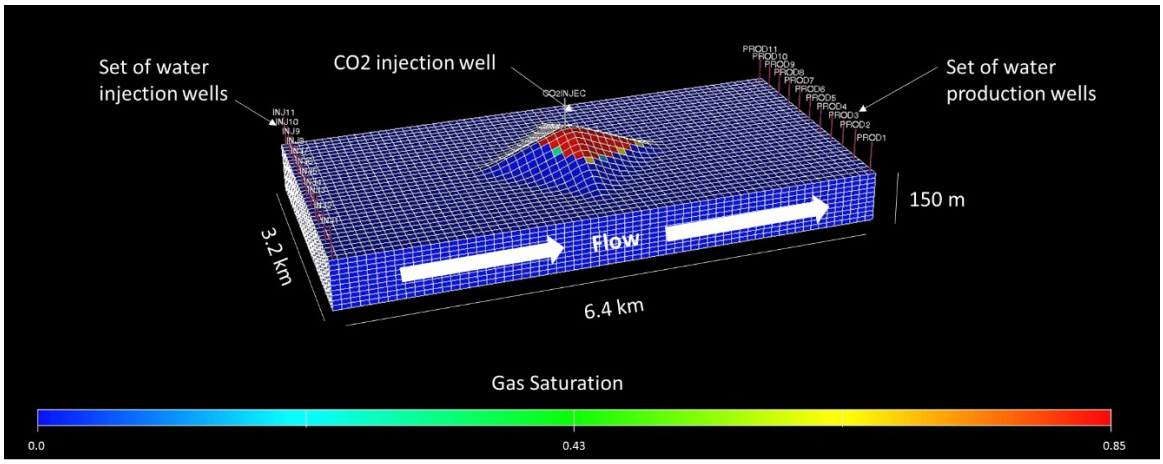

Figure 3: The figure shows the model setup and resulting CO_2 saturations: 11 water injection wells and 11 water production wells create a constant horizontal variation in overpressure across the model. CO_2 is injected via a CO_2 injection well into the upper two cells in the centre of the anticline.

Representative Paleocene reservoir properties from the North Sea were used to populate the reservoir model. The horizontal and vertical permeability is 25 and 12.5 mD, respectively, and the porosity is 20 % (Jones et al., 2003). The salinity is 0.1 kg/l. Relative permeability for the aqueous phase was calculated using the method introduced by van Genuchten (1980) with constants taken from Pruess et

al. (2003; Figure 4). The relative permeability for super-critical CO_2 was calculated after Corey (1954). Irreducible water saturation and critical gas saturation were set to 0.139 and 0.05 respectively (Pruess et al., 2003). Capillary pressure was ignored following Dennis et al. (2000) who concluded that the effect of capillary pressures in a reservoir scale simulation was negligible when compared to the hydrodynamic effects.

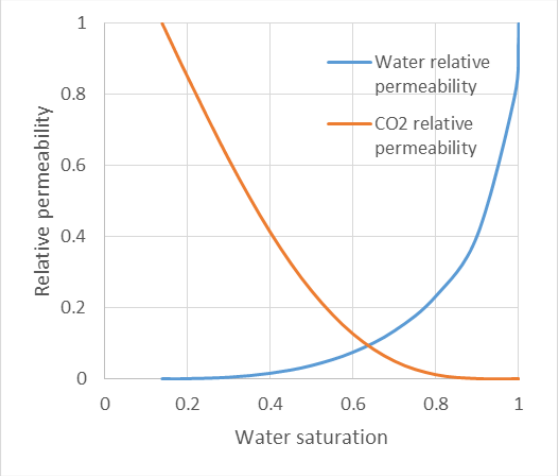

Figure 4: The relative permeability curves.

CO_2 density was calculated using the Redlich-Kwong EoS (Redlich & Kwong, 1949) with coefficients suggested by Spycher et al. (2003). Viscosity of CO_2 was calculated using a linear regression introduced by Mathias et al. (2010). Brine density and viscosity were calculated using Batzle & Wang (1992). The mutual dissolution of brine and water was calculated using the solubility model introduced in Spycher et al. (2003, 2005).

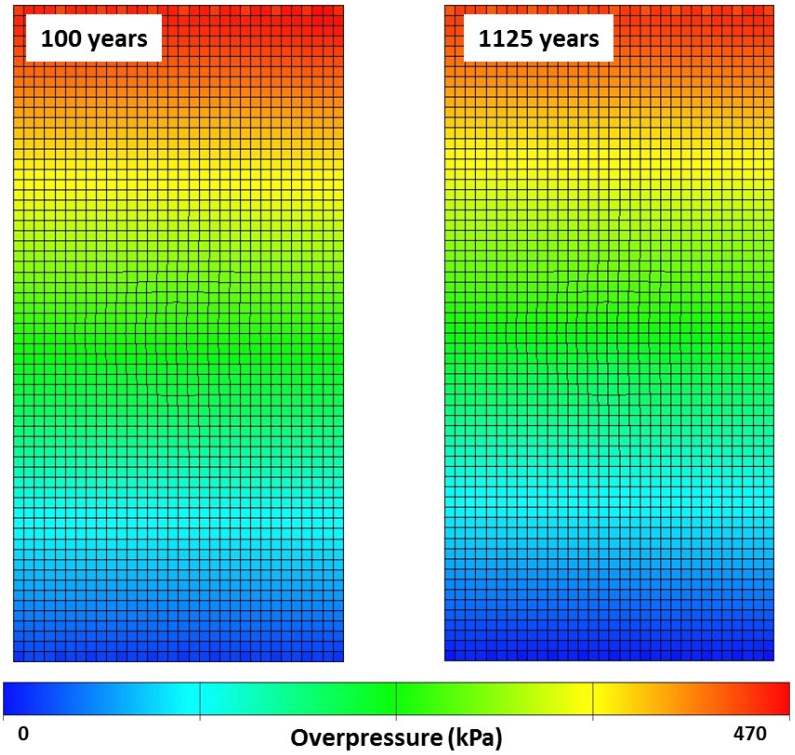

Figure 5: The Z-slice through model layer 6 shows the overpressure of the aqueous phase relative to a hydrostatic gradient defined by the pressure sink in the model. The overpressure distribution is similar before CO_2 injection starts (100 years) and when the simulation stops (1125 years). The calculated horizontal variation in overpressure of the shown model is 72 kPa/km throughout the model for most of the running time except in the vicinity of the brine injection wells. However, during the time of CO_2 injection and shortly after, the horizontal variation in overpressure is higher.

The simulation runs for 1125 years. The brine injection and production wells operate constantly to maintain a constant pressure field (Figure 5). After 100 years the overpressure distribution has reached a steady state, then CO_2 injection starts at a rate of 0.13 Mt/yr and lasts for 25 years. After CO_2 injection has ceased, the model runs for additional 1000 years with the brine injection and production wells continuing. Pressure is higher and hydrodynamic flow is temporally altered during the CO_2 injection period and shortly after due to the addition of the CO_2 volumes. However, this is expected and occurs in real CO_2 injection operations.

Several models were run: One base case which represents a nearly hydrostatic aquifer (a horizontal variation in overpressure of 0.6 kPa/km) and several hydrodynamic models with different brine injection rates. The nearly hydrostatic aquifer is not entirely hydrostatic (0 kPa/km) because it was necessary to keep both the brine injection and the production wells running to create results comparable with the hydrodynamic cases. A horizontal variation in overpressure of 0.6 kPa/km would be difficult to detect in a natural reservoir and is well within the range of uncertainty of the investigation of hydrodynamic systems. The different hydrodynamic models presented in this study are named according to their horizontal pressure gradients. In this study, the pressure gradient was calculated based on pressure data from one extent of the model to the other in the long direction. Horizontal variations in overpressure were found to be consistent throughout the model. Vertical pressure changes outside the expected hydrostatic pressure increase with depth were negligible.

4.2. Results

The injection of CO_2, the development of the CO_2 plume and the dissolution of CO_2 into brine has been investigated in many studies (e.g. Ghanbari et al., 2006; Heinemann et al., 2012; Peters et al., 2015). Figure 6 shows that when injected into the hydrostatic model, the CO_2 remains in the top of the anticline with a nearly horizontal FWL. When injected into the hydrodynamic model, the FWL tilts towards the water production wells. The stronger the pressure gradient, the greater the tilt. With a horizontal variation in overpressure of 180 kPa/km, the tilt is so strong that CO_2 starts migrating out of the anticline. Here, the CO_2 leaves the structural closure approximately 150 years after injection has ceased, at a time when CO_2 accumulations in hydrostatic simulations are already reducing due to the dissolution of CO_2 into brine. This may not be anticipated in a real CO_2 storage operation and shows the importance of a hydrodynamic analysis to prevent undesired CO_2 migration.

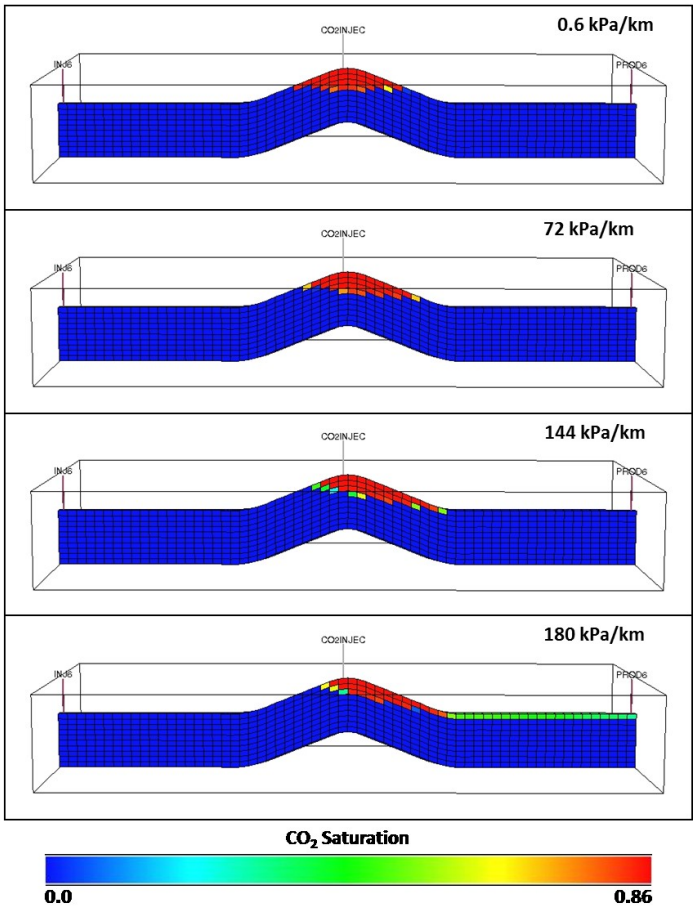

Figure 6: Middle X-Z plane of the reservoir model showing the CO_2 saturation after 1125 years. Brine flows from the left to the right. Whereas no horizontal variation in overpressure leads to a horizontal CO_2-water contact, a horizontal variation in overpressure tilts the contact. With a horizontal variation in overpressure of 180 kPa/km, the tilt triggers the CO_2 to leave the anticline. Vertical exaggeration is 4.

Figure 7 shows the dissolved CO_2 in the brine after 1125 years. There is significant CO_2 dissolution where free CO_2 is present because the brine and the CO_2 are in direct contact. Here, the mole fraction of the CO_2 in the brine is higher than anywhere else in the aquifer (Figure 7). The brine below the gas cap is partially saturated with CO_2 and has started sinking to the base of the aquifer. In the nearly hydrostatic model (0.6 kPa/km), a dissolution pattern showing sinking CO_2-saturated brine has established which enhances dissolution in saline aquifers. However, the cell size is not sufficiently small to resolve potential natural convection of CO_2-saturated brine. In the chosen scenario, such

convection would be expected to start after the post-injection time of 1000 years (using Riaz et al., 2006). Hence, the observed convection and dissolution rates are mainly an effect of numerical dispersion (see e.g. Emami-Meybodi et al. (2015) for more information). In a hydrodynamic system, saturated brine sinks and is simultaneously diverted towards lower overpressure. The stronger the horizontal variation in overpressure, the further the partially saturated brine is diverted.

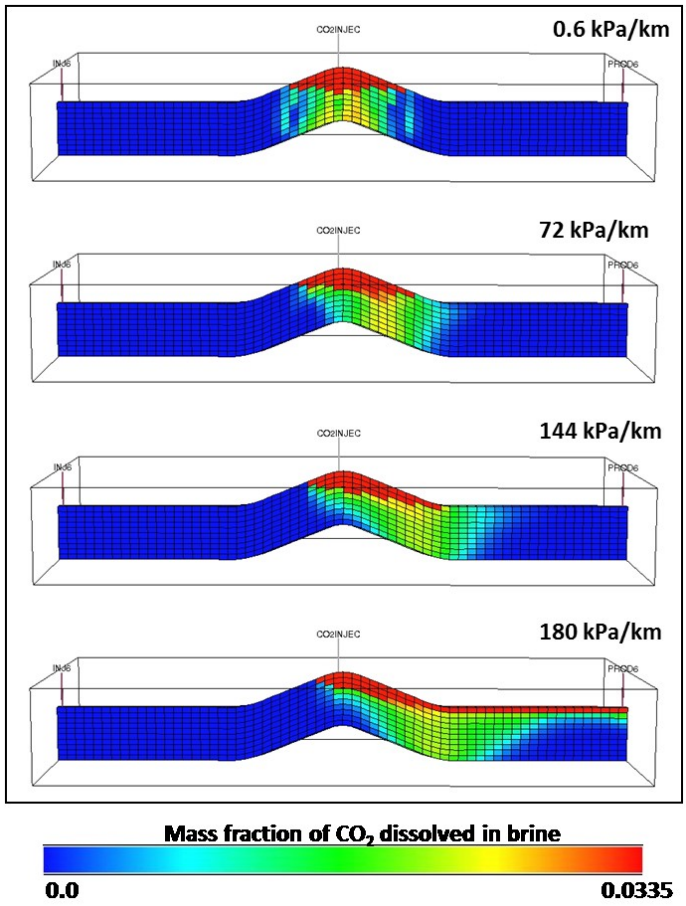

Figure 7: Middle X-Z plane of the reservoir model showing the CO_2 dissolved in the water phase after 1125 years. Brine flows from the left to the right. When no hydrodynamic flow is present, CO_2 and brine create a convective system allowing CO_2-saturated brine to sink and unsaturated brine to rise to the CO_2-water contact. With the added component of a horizontal variation in overpressure, CO_2-saturated brine is transported away from the CO_2-water contact allowing for more interaction between unsaturated brine and CO_2 thus further enhancing CO_2 dissolution. With a horizontal variation in overpressure of 180 kPa/km, the tilt triggers the CO_2 to leave the anticline and the CO_2 dissolution is even higher. Vertical exaggeration is 4.

Figure 8 shows the volume of dissolved CO_2 in all cases modelled. The highest dissolution rates are achieved during the injection and shortly after the injection periods when CO_2 is still mobile and distributed over many cells before it settles underneath the caprock. During this period, the results show that there is hardly any difference in dissolution rates between injection into a hydrostatic and a hydrodynamic aquifer. Here, the buoyancy forces of the CO_2, which determine the ascent of the CO_2 to the caprock, are dominant and the lateral flow in the reservoirs modelled in this study has no significant effect on the emplacement of the CO_2 underneath the caprock (~2 % increase in dissolution in the 180 kPa/km model compared to the hydrostatic model). With 3.25 Mt of injected CO_2 after 25 years, approximately 8.5% of the CO_2 has dissolved by the end of the injection period. During the post injection period the continued effectiveness of dissolution as a trapping mechanism is more significantly related to the strength of the horizontal variation in overpressure.

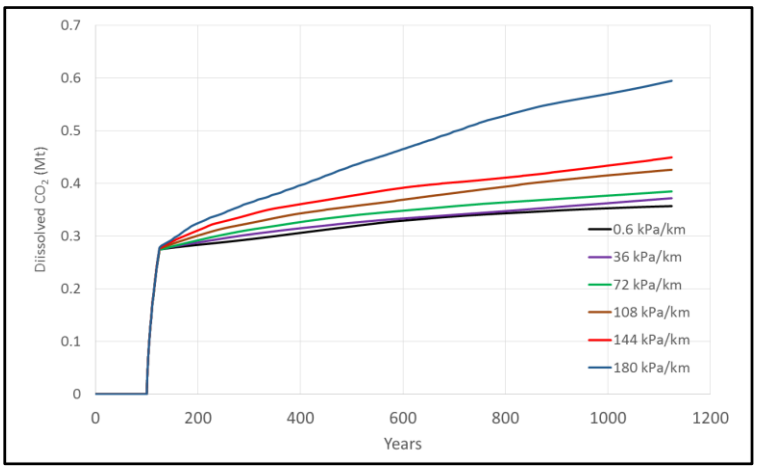

Figure 8: The amount of dissolved CO_2 for the hydrostatic model (0.6 kPa/km) and several hydrodynamic scenarios. The dissolution rate is greatest during the injection phase when CO_2 enters brine-saturated cells. The amount of dissolved CO_2 is roughly similar for all models during the injection period. After the injection period, CO_2 gradually dissolves into the pore water. The greater the horizontal variation in overpressure in the aquifer, the more CO_2 dissolves. When CO_2 migrates out of the anticline due to the tilt, the dissolution rate increases dramatically (180 kPa/km; solid blue line).

4.3. Discussion

The tilt of the FWL is only determined by the horizontal variation in overpressure and the density difference of the fluid phases. The increase of the CO_2 dissolution due to hydrodynamic flow is mainly a function of the brine flow removing CO_2-saturated brine away from the CO_2-brine interface. Hence, the increase of the dissolution rate is a function of the lateral brine flow rate. The flow rate of brine and the horizontal variations in overpressure are connected linearly via Darcy's law, providing density changes due to dissolution are not significant (Figure 9). The slightly higher average pressures in simulations with higher horizontal variations in overpressure can be neglected in terms of their impact on dissolution. Firstly, the average pressure differences are small (484 kPa difference between the 144 kPa/km and the nearly hydrostatic model), and secondly, the main pressure differences between the scenarios occur close to the water injection wells, hence in an area where no CO_2 dissolution takes place.

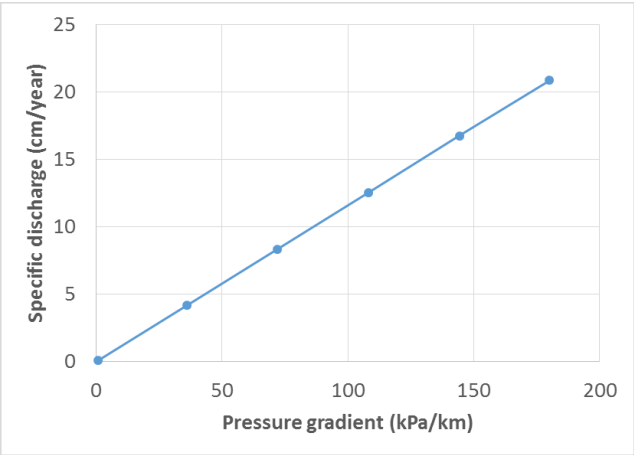

Figure 9: Linear relationship between the horizontal variation in overpressure and specific discharge in the simulations conducted for this study. The flow was measured near both ends of the model after 1125 years. However, the flow near and underneath the anticline is generally higher due to the presence of CO_2.

The absolute amount of dissolved CO_2 with time is dependent on many parameters and will not be discussed here any further. Instead, the mass of dissolved CO_2 in the nearly hydrostatic model was regarded as a baseline. The dissolved CO_2 from hydrodynamic models were plotted against this baseline to quantify the effect of hydrodynamic flow on CO_2 dissolution (Figure 10). The graph shows that the stronger the horizontal variation in overpressure, the higher the dissolution rate.

Under the specific model setup and the chosen parameters and after a post injection period of 1000 years, approximately 27 % more CO_2 will dissolve in a hydrodynamic aquifer with a horizontal variation in overpressure of 144 kPa/km compared to a hydrostatic scenario. The increase of the dissolution rate in hydrodynamic aquifers increases with time. Hence the longer the CO_2 remains in a hydrodynamic aquifer, the greater the dissolution relative to the hydrostatic case.

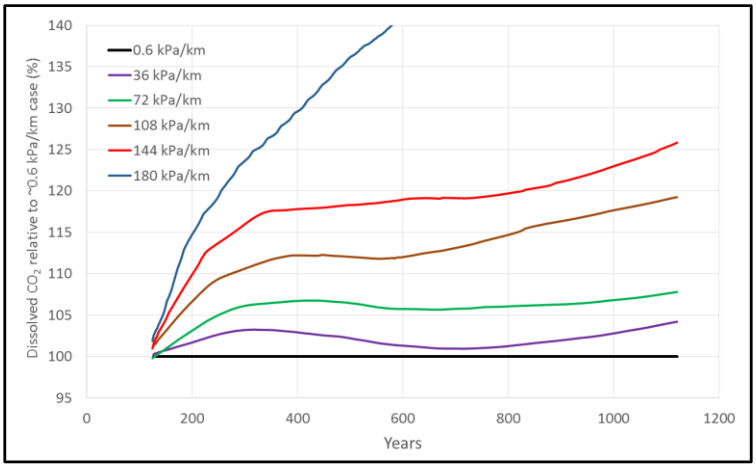

Figure 10: The amount of dissolved CO_2 relative to the hydrostatic base case (0.6 kPa/km); solid black line) after CO_2 injection ceased. After a post injection period of 1000 years, more than 20 % more CO_2 will dissolve in an aquifer with a horizontal variation in overpressure of 144 kPa/km.

The model results indicate a distinctive increase in dissolution relative to the hydrostatic case during the first 200 years after CO_2 injection has ceased. This is a result of a rapid increase in dissolved CO_2 in the aquifer (Figure 11). 'The aquifer' is here defined as brine-filled cells with no gaseous CO_2 compared to brine filled cells with a gas saturation greater than 0. The rapid increase in 'dissolved CO_2 in the aquifer' in the hydrodynamic model relative to the nearly hydrostatic model (Figure 11)

during the first 200 years after injection has ceased falls within the time period of the main redistribution of the CO_2 plume. While tilting, the supercritical CO_2 enters new cells in the direction of flow which quickly become saturated. At the same time, the plume leaves behind CO_2 saturated brine filled cells which count as 'dissolved CO_2 in the aquifer' once the incoming fresh brine has dissolved the residual CO_2. The nearly hydrostatic model has no tilting and hence does not show this effect.

Generally, high rates of dissolution into the aquifer occur when CO_2-saturated brine starts sinking and is replaced by fresh brine. The hydrodynamic flow enhances this process by introducing more unsaturated brine at the base of the CO_2 accumulation. The dissolution enhancing effect of this process is dependent on the hydrodynamic flow rate and therefore dependent on the horizontal variation in overpressure.

The '180 kPa/km' model shows very high dissolution rates. As mentioned before, in this scenario CO_2 has migrated out of the anticline due to the strong tilt. As seen in Figure 6, supercritical CO_2 migrates along the top of the aquifer towards the production wells. By doing this, the CO_2 occupies new brine filled cells which leads to a very effective dissolution process. Additionally, saturated brine is being removed from the CO_2-brine interface.

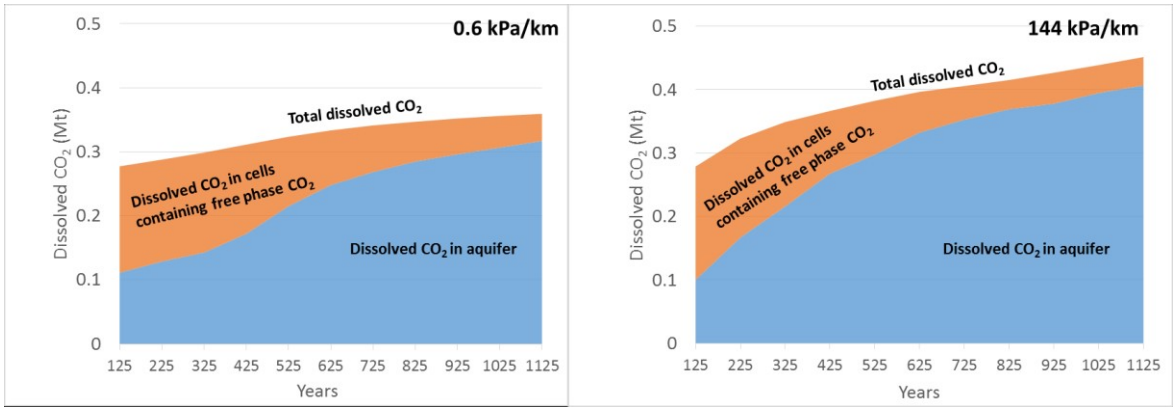

Figure 11: The figures show the total amount of dissolved CO_2, the amount of dissolved CO_2 in the aquifer (blue) and the amount of dissolved CO_2 in cells containing free phase CO_2 (brown) for the hydrostatic case (left) and the hydrodynamic case with a horizontal variation in overpressure of 144 kPa/km (right). Solubility trapping is more effective when CO_2 is injected into hydrodynamic aquifer. There is a rapid increase in CO_2 dissolved into the aquifer in hydrodynamic cases compare to the hydrostatic case during the first 300 years after injection has ceased.

5. Conclusions

Horizontal variations in overpressure in hydrodynamic aquifers will tilt CO_2-water FWL to a similar degree as they tilt oil-water FWL because CO_2 will be present as a supercritical phase with densities comparable to the density of oil. That means for a CO_2 storage operation that possible hydrodynamic spill points have to be mapped out to avoid fluid migration out of the intended storage site due to the tilt. Depending on the reservoir architecture, the effect of hydrodynamic flow on CO_2 storage can be negative (less storage capacity) and horizontal variations in overpressure have to be taken into account for a storage capacity calculation based on structural spill points.

Hydrodynamic flow should be taken into account when a CO_2 storage operation is planned and designed. Therefore, the possible presence of hydrodynamic flow has to be investigated prior to

injection to modify the storage capacity estimation. This is of particular importance when targeting dome structures in saline aquifers where no hydrocarbons and consequently no tilted pre-injection FWLs are present to indicate hydrodynamic flow.

Once the CO_2 has been injected into an aquifer, CO_2 starts dissolving into the brine. When injected into a hydrodynamic aquifer, the dissolution rate is increased because brine saturated with CO_2 will be removed more effectively from the CO_2-brine interface and more unsaturated brine comes into contact with the CO_2. This increase in dissolution is scenario-dependent but simulations conducted for this study suggest an increase of more than 20 % for a post-injection period of 1000 years in an aquifer with a horizontal variation in overpressure of 144 kPa/km. The simulation results suggest that the dissolution rate will continue to increase with time relative to a hydrostatic aquifer.

Hydrodynamic flow in a reservoir which is targeted for CO_2 storage requires a higher degree of understanding but research on oil reservoirs has proven that it is a parameter that can be understood and accounted for. The faster reduction of free CO_2 reduces the risk of leakage and also reduces the pressure on the cap-rock. Hence by increasing the CO_2 dissolution rate the presence of hydrodynamic flow increases storage security.

Acknowledgements

Thanks to Schlumberger for the use of the Eclipse reservoir simulation software.

6. References

Bachu, S. & Underschultz, J.R., 1993. Hydrogeology of formation waters, North eastern Alberta Basin. AAPG Bulletin, 77/10, 1745-1768.

Batzle, M. & Wang, Z., 1992. Seismic properties of pore fluids. Geophysics, 57, 1396–1408.

Birch, P. & Haynes, J., 2003. The Pierce Field, Blocks 23/22a, 23/27, UK North Sea. Geological Society, London, Memoirs, 20, pp.647–659.

Bjoerlykke, K., 1997. Lithological control on fluid flow in sedimentary basins. In: B. Jamtveit (ed), Fluid Flow and Transport in Rocks — Mechanisms and Effects. Chapman and Hall, London, 15-34.

Cayley, G.T., 1987. Hydrocarbon migration in the Central North Sea. In: J. Brooks and K. Glennie (eds), Petroleum Geology of NW Europe. Graham and Trotman, London, 549-555.

Dennis, H., Baillie, J., Holt, T. & Wessel-Berg, D., 2000. Hydrodynamic activity and tilted oil-water contacts in the North Sea. In: K. Ofstad, E.J. Kittilsen, P. Alexander-Marrack (eds), Improving the Exploration Process by Learning from the Past. NPF Special Publications, 9, 171–85.

Dennis, H., Bergmo, P. & Holt, T., 2005. Tilted oil-water contacts – modelling the effects of aquifer heterogeneity. In: A.G. Dore, B. Vinning (eds), Petroleum geology: North-West Europe and Global Perspectives. Proceedings of the 6th Petroleum Geology Conference. The Geological Society, London.

Ghanbari, S., Al-Zaabi, Y., Pickup, G.E., Mackay, E., Gozalpour, F. & Todd, A.C., 2006. Simulation of CO_2 storage in saline aquifers. Chemical Engineering Research and Design, 84, 764-775.

Green, S., Swarbrick, R.E. & O'Connor, S., 2014. The importance of recognizing hydrodynamics for understanding reservoir volumetrics, field development and well placement. Paper OTC 25150 presented at the Offshore Technology Conference, Houston, Texas.

Emami-Meybodi, H., Hassanzadeh, H., Green, G.P. & Ennis-King, J., 2015. Convective dissolution of CO_2 in saline aquifers: Progress in modelling and experiments. International Journal of Greenhouse Gas Control, 40, 238-266.

Ennis-King, J. & Paterson, L., 2005. Role of convective mixing in the long-term storage of carbon dioxide in deep saline formations. SPE Journal, 10/3, 349–356.

Heinemann, N., Wilkinson, M., Pickup, G.E., Haszeldine, R.S. & Cutler, N., 2012. CO_2 Storage in the offshore UK Bunter Sandstone Formation. International Journal of Greenhouse Gas Control, 6, 210-219.

Hubbert, M.K., 1953. Entrapment of petroleum under hydrodynamic conditions. AAPG Bulletin, 37, 1954-2026.

Hubbert, M.K., 1967. Application of hydrodynamics to oil exploration. Proceedings of the 7th World Petroleum Congress, lb, 59-75.

IPCC, 2005. In: B. Metz, O. Davidson, H.C.D Coninck, M. Loos, L.A. Meyer (eds), IPCC Special Report on Carbon Dioxide Capture and Storage. Cambridge University Press, Cambridge.

IPCC, 2014. Climate Change 2013- The Physical Science Basis, Available at: http://www.ipcc.ch/report/ar5/wg1/.

Jones E., Jones R., Ebdon C., Ewen D., Milner P., Plunkett J., Hudson G., Slater G., 2003. The Millennium Atlas: Petroleum geology of the central and northern North Sea, Eocene, eds Evans D., Graham C., Armour A., Bathurst P. (Geological Society, London), 261–277

Lindeberg, E., Zweigel, P., Bergamo, P., Ghaderi, A. & Lothe, A., 2000. Prediction of CO_2 distribution pattern improved by geology and reservoir simulation and verified by time lapse seismic. 5th International Conference on Greenhouse Gas Control Technologies, Cairns, Australia.

Lovell, B., 2011. Challenged by Carbon: The Oil Industry and Climate Change. Department of Earth Sciences, University of Cambridge, 211 pp.

Mathias, S.A., Hardisty, P.E., Trudell, M.R. & Zimmerman, R.W., 2010. Erratum to "Screening and selection of sites for CO_2 sequestration based on pressure buildup". International Journal of Greenhouse Gas Control, 4/1, 577-585.

Megson, J. B., 1992. The North Sea Chalk play: examples from the Danish Central Graben. In: R.F.P. Hardman (ed), Exploration Britain: Geological Insights for the Next Decade. Geological Society, London, Special Publications, 67, 247–282.

Melnik, A. & Rostron, B.J., 2011. Petroleum hydrogeology of Southwestern Saskatchewan. Search and Discovery Article #80189.

O'Connor, S., Swarbrick, R.E. & Jones, D., 2008. Where has all the pressure gone? Evidence from pressure reversals and hydrodynamic flow. First Break, 26, 55–61.

O'Connor, S., Rasmussen, H., Swarbrick, R. & Wood, J., 2011. Integrating a hydrodynamically-tilted OWC and a salt-withdrawal depositional model to explore the Ula Trend. Geofluids, 11, 388-400.

Peters, E., Egberts, P.J.P., Loeve, D. & Hofstee, C., 2015. CO_2 dissolution and its impact on reservoir pressure behaviour. International Journal of Greenhouse Gas Control, 43, 115-123.

Pruess, K., Xu, T., Apps, J. & Garcia, J., 2003. Numerical modelling of aquifer disposal of CO_2. SPE Journal, 8/1, 49–60.

Riaz, A., Hesse, M., Tchelepi, H.A. & Orr, F.M., 2006. Onset of convection in a gravitationally unstable diffusive boundary layer in porous media. Journal of Fluid Mechanics, 548, 87–111.

Robertson, J., Goulty, N.R. & Swarbrick, R.E., 2013. Overpressure distribution in Palaeogene reservoirs of the UK Central North Sea and implications for lateral and vertical flow. Petroleum Geoscience, 19, 223-236.

Redlich, O. & Kwong, J.N.S., 1949. On the thermodynamics of solutions. V. An equation of state. Fugacities of gaseous solutions. Chemical Reviews, 44, 233–244.

Setzmann, U. & Wagner, W., 1991. A new equation of state and tables of thermodynamic properties for methane covering the range from the melting line to 625 K at pressures up to 1000 MPa. Journal of Physical and Chemical Reference Data**,** 20/6, 6, 1061-1151.

Span, R. & Wagner, W., 1996. A new equation of state for carbon dioxide covering the fluid region from the triple-point temperature to 1100 K at pressures up to 800 MPa. Journal of Physical and Chemical Reference Data**,** 25/6, 1509–1596.

Spycher N., Pruess K. & Ennis-King J., 2003. CO_2-H_2O Mixtures in the geological sequestration of CO_2. I. Assessment and calculation of mutual solubilities from 12 to 100°C and up to 600 bar. Geochimica et Cosmochimica Acta, 67, 3015–3031.

Spycher N. & Pruess K., 2005. CO_2-H_2O Mixtures in the geological sequestration of CO_2. II. Partitioning in chloride brines at 12-100°C and up to 600 bar. Geochimica et Cosmochimica Acta, 69, 3309–3320.

Swarbrick, R.E. & Osborne, M.J., 1997. Mechanisms which generate abnormal pressures: an overview. In: B.E. Law, G.F. Ulmishek, V.I. Slavin (eds), Abnormal Pressures in Hydrocarbon Environments. AAPG Memoirs, 70, 13-53.

Thomasen, J. B. & Jacobsen, N. L. 1994. Dipping fluid contacts in the Kraka Field, Danish North Sea. Paper SPE 28435 presented at the 69th Annual SPE Technical Conference, New Orleans, Luisianna.

Tozer, R.S. & Bothwick, A.M., 2010. Variation in fluid contacts in the Azeri firld, Azerbeijan: Sealing faults of hydrodynamic aquifer? In: S.J. Jolley, Q.J. Fisher, R.B. Ainsworth, P.J. Vrolijk, S. Delisle (eds), Reservoir compartmentalization. Geological Society, London, Special Publication, 347, 103-112.

Van Genuchten, M.T., 1980. A closed-form equation for predicting the hydraulic conductivity of unsaturated soils. Soil Science Society of America Journal, 44, 892–898.

Zhou, Q., Birkholzer, T.B., Tsang, C. & Rutqvist, J., 2008. A method for quick assessment of CO_2 storage capacity in closed and semi-closed saline formations. International Journal of Greenhouse Gas Control, 2, 626-639.